TÜBİTAK

Turkish Journal of Physics

http://journals.tubitak.gov.tr/physics/

Research Article

Turk J Phys
(2017) 41: 477 – 490

doi:10.3906/fiz-1704-25

Deconvolution analysis of thermoluminescent glow curves in various commercial dosimeters using two different approaches in the framework of the one-trap, one-recombination model

Eren ŞAHİNER*
Institute of Nuclear Sciences, Ankara University, Ankara, Turkey

Received: 24.04.2017 • **Accepted/Published Online:** 26.07.2017 • **Final Version:** 18.12.2017

Abstract: This paper reports kinetic analysis on the thermoluminescence (TL) glow peaks of various widespread luminescence dosimeters. A common general order kinetic (GOK) approximation and a relatively recently suggested Lambert W-function equation were used. The activation energies and the order of kinetic parameters are the main subjects of the present study. According to the results of this study, the activation energies of the main dosimetric peaks are estimated as 2.05 ± 0.11, eV, 1.23 ± 0.05 eV, and 1.11 ± 0.06 eV for LiF based dosimeters (TLD100, TLD600, TLD700), Al_2O_3:C (TLD500), and BeO dosimeters, respectively. Moreover, a number of other peaks were deconvolved and investigated in terms of kinetic parameters and frequency factors. Additionally, the advantages of the Lambert equation, being completely analytical, are reported and compared to those of the GOK method while deconvolving TL glow curves. The results of this study suggest that the Lambert W-function is promising in revealing the physical meaning of trap-charge and recombination mechanisms for the characterization of materials throughout physical-based sciences.

Key words: Deconvolution, thermoluminescence (TL), general order kinetic (GOK), Lambert W-function

1. Introduction

Optically stimulated luminescence and thermoluminescence (OSL and TL, respectively) are supplementary forms of the luminescence phenomenon, which is based on trapped charge movements inside the crystal. Luminescence can be used in many research fields such as accidental and personal dosimetry, dating of terrestrial materials, and characterization of solids. TL can be observed when a previously irradiated solid is subjected to thermal stimulation, being different from light spontaneously emitted from a substance when it is heated to incandescence (also arising with temperature in excess of 200 °C). Therefore, luminescence emission can occur within three sequential steps in any material. Firstly, trap-charge mechanisms have to work in the material tolerating higher temperatures around a couple of hundred degrees centigrade. Secondly, the material must have absorbed energy due to exposure to ionizing radiation at a suitable time in the past. Lastly, the luminescence emission is stimulated by heating the material, mostly linearly [1,2]. Detection of this emission can be carried out roughly with several instrumentation combinations using phototubes, sensitive heater units, and sample holder magazines. Both mathematical explanation and physical meaningfulness, however, require considerable efforts in further study. Following intense experimental research over the past decades, modelling approaches have been adopted in order to clarify this phenomenon in the literature. According to the one-trapping,

*Correspondence: sahiner@ankara.edu.tr

one-recombination center (OTOR hereafter) model, various approaches are established, as retrapping may or may not occur. Consequently, first-, second-, and general-order kinetics (GOK) can take place, namely no retrapping, 50% retrapping, and moderate retrapping, respectively [3–6]. Furthermore, all the aforementioned kinetic models are analytically solved by Kitis et al. [7], which has been well described and used in a wide range of luminescence materials, both man-made and natural [8,9].

Another drastic approach has recently been suggested for general semianalytical expressions for TL, OSL, and other luminescence stimulation modes derived from the OTOR model using the Lambert W-function [10]. This function has some advantages, especially when the retrapping probability becomes greater than the recombination probability, which remains a problem of all analytical peak model expressions. Specifically, these authors have discovered that the same equation, with slight modifications, can explain TL, isothermal TL, continuous wave optical stimulated luminescence (CW - OSL), linearly modulated OSL (LM - OSL), and TL measured using different heating rates as well as exponential heating.

Although the related theory is thoroughly established, the literature so far lacks manuscripts dealing with applications of the Lambert W-function [11]; this novel approach was applied for various TLD100 types, with different origins, and the results indicated that the glow-curve structure and the kinetic parameters of the TLD100s are identical. Moreover, Kitis et al. [12] have suggested isothermal decay of TL in MgB_4O_7:Dy, Na and LiB_4O_7:Cu using the Lambert W-equation towards discriminating between radiative delocalized and radiative localized recombination processes. However, for all the above-mentioned works, the approximation of the Lambert equation still needs more tests with different dosimeters.

For this purpose, the aim of the present work is twofold: firstly, to deconvolve experimental data consisting of various TL glow curves that were obtained from widespread synthetic dosimetric crystals using both the GOK and Lambert W-function, and, secondly, to compare the parameters of deconvolution analysis, examining the effective employment of the Lambert W-function in the trap-charge and recombination mechanisms of crystals. Further, the properties of the high-temperature peaks of LiF-based dosimeters were investigated and compared in detail.

2. Materials and methods

All experiments were carried out using a Riso TL/OSL-DA-20 reader equipped with a $^{90}Sr/^{90}Y$ beta source, delivering a nominal dose rate of 0.130 $\pm$ 0.003 Gy/s. A 9635QA photomultiplier tube combined with a Hoya-U340 filter was used for detection of luminescence emissions. All measurements were conducted in a nitrogen atmosphere with low constant heating rate of 1 $^{\circ}$C/s in order to avoid significant temperature lag. Samples were heated to the maximum temperature of 400 $^{\circ}$C using stainless steel cups. LiF-based dosimeters (TLD100, TLD600, and TLD700), Al_2O_3:C (TLD500), and BeO commercial dosimeters were used and all were resettled before irradiation. Finally, popular commercial spreadsheet software was used for the deconvolution of TL glow curves.

All the aforementioned dosimeters have been systematically employed among personnel and neutron dose monitoring research and applications. In particular, low temperature peaks are very well known with significant reproducibility in the relevant literature as well as kinetic parameter values. On the other hand, high temperature peaks play an important role in TL dosimetry, mostly due to their long lifetimes. The LiF-based dosimeters used in the present work with dimensions of 3.2 $\times$ 3.2 $\times$ 0.89 mm^3 were purchased from Harshaw. The Al_2O_3:C dosimeter-chips (dimensions 0.6 cm in diameter and 0.2 cm in height) obtained from Landauer Inc., Stillwater Crystal Growth Division (USA), were doped with carbon (Al_2O_3:C, TLD500). Lastly, BeO

ceramics were obtained from Thermolax 995, Brush Wellman Inc., USA, in the form of chips, with dimensions of 4 mm in diameter and thickness of 1 mm.

2.1. TL glow curve shapes and deconvolution

2.1.1. GOK model

The first- and second-order kinetics of the TL equation have been developed with the use of particular simplifying assumptions that have been deeply discussed in the literature by different authors [13–15]. Nevertheless, for cases where these assumptions might not work, May and Partridge [6] have used an empirical expression for general-order TL kinetics, termed the GOK model. A semianalytical solution was suggested by Kitis et al. [7] in terms of maximum peak intensity I_m and the maximum peak temperature T_m.

TL glow curve deconvolution, especially when coupled with the ability to separate different overlapping trapping states, has been shown to be of great importance [16]. Consequently, the computerized glow curve deconvolution (CGCD) analysis in TL research is a well-established and successfully applied diagnostic tool. Kitis et al. [7] proposed the single glow-peak equations of GOK, which can be used in the case of discrete trap distributions as in the present study:

$$I(T) = I_m \cdot b^{\frac{b}{b-1}} \exp\left(\frac{E}{kT}\frac{T-T_m}{T_m}\right) \cdot \left[(b-1)(1-\Delta)\frac{T^2}{T_m^2}\exp\left(\frac{E}{kT}\frac{T-T_m}{T_m}\right) + \mathrm{Z}_m\right]^{-\frac{b}{b-1}}, \tag{1}$$

where

$$\Delta = 2kT/E, \Delta_m = 2kT_m/E and Z_m = 1 + (b-1)\cdot\Delta_m \tag{2}$$

while the frequency factor can be estimated with the rearranging of Eq. (3)

$$s = \frac{\beta E}{kT_m^2\left(1 + 2kT_m(b-1)/E\right)} \exp\left(\frac{E}{kT_m}\right) \tag{3}$$

Although this model could be used for high-level fit accuracy, it is solely an empirical equation and so is not associated with a physical model [17]. Thus, is some cases GOK parameters obtained from CGCD analysis might display contradictions from author to author. Additionally, higher b values could lead to problematic descriptions.

2.1.2. Lambert W-function

As an alternative to the GOK model, the Lambert equation was meticulously solved by Kitis and Vlachos [10]; fitting of the glow peaks can be achieved through $1 < \mathrm{R}$ and $1 > \mathrm{R}$, in which $\mathrm{R} = \mathrm{A}_n/\mathrm{A}_m$ is the trapping–recombination factor ratio. Furthermore, unlike the GOK equation, which is semianalytical, Lambert equations were yielded based on a completely analytical model. In addition, these authors, having improved the deconvolution analysis, [18] concluded that all the glow peaks of different dosimeters might be fitted with the equation related to $\mathrm{R} < 1$. Eventually, for the linear heating rate, the functions (Eqs. (4)–(8)) of the Lambert approach were presented by Sadek et al. [11,19].

$$I = I_m \frac{W\left[\exp\left(Z_m\right)\right] + W\left[\exp\left(Z_m\right)\right]^2}{W\left[\exp\left(Z\right)\right] + W\left[\exp\left(Z\right)\right]^2} \exp\left(-\frac{E}{k}\left(\frac{1}{T} - \frac{1}{T_m}\right)\right), \tag{4}$$

where k is Boltzmann coefficient, E is activation energy, $R = A_n/A_m$, and $W[e^z]_{TL}$ the values of $W[e^z]$ for z given by

$$z = \frac{1}{c} - \ln(c) + \frac{E \exp\left[\frac{E}{kT_m}\right]}{kT_m^2 F_{TL1}(1-R)} F(TE) \tag{5}$$

$$F_{TL1} = \frac{-1.05R^{1.26} + 1}{(1-R)} \tag{6}$$

$$c = \frac{n_0 R}{N(1-R)} \tag{7}$$

$$\frac{\beta E}{kT_m^2} = F_{TL} s \exp\left(-\frac{E}{kT_m}\right) \tag{8}$$

According to Sadek et al. [11,19], changing the n_o/N did not affect the value of the calculated E so long as $R < 1$. For $tA_n < A_m$ the form of this equation is $R < 1$ and so $c > 1$. In contrast, for $A_n > A_m$ the form of this equation is $R > 1$ and so $c < 1$. These two cases should be investigated separately [19,20]. Moreover, these equations have some advantages for the GOK and the mixed-order kinetics (MOK) equations' determination of the activation energies of TL peaks. Lastly, the goodness of fit in all component resolved analysis was tested by the figure of merit (FOM) of Balian and Eddy [21].

3. Results and Discussion

Using both models, the deconvolution of glow curves of TLD100, TLD600, and TLD700 dosimeters using the peak maximum intensity I_m and peak maximum position T_m is shown in Figures 1–3. For the aforementioned materials, peaks 1–5 are common peaks in all LiF-based dosimeters; all corresponding parameters are presented in the first three columns of Tables 1 and 2, respectively. It is clear that the whole glow curve could be divided into two temperature regions, one consisting of the region up to peak 5 and the other including all other high-temperature peaks. Furthermore, peak 5 is indispensable in terms of its yielded dosimetric properties. It can be seen that the energy values of this peak are around 2 eV if all dosimeters are taken into account for an average evaluation.

The energies of the first temperature region (<300 °C) are compatible with those presented by Sadek et al. [11]. On the other hand, it is clear that the structure of the second region (>300 °C), which is significant for both neutron as well as high dose dosimetry, yields a structure that is sample dependent. The eighth peak of TLD100 could not be observed in the other dosimeters' glow peaks. In the high-temperature area, glow peaks of LiF-based dosimeters consist of three overlapped glow peaks, including some parts of peak 5, which is regarded as 5a in the literature (peak 6 in Figures 1–3) [11,22]. The contribution of peak 5 from close peaks might be problematic when evaluating dose exposures. In particular, at low dose levels and under the usual annealing procedures, the interference from peak 4 accounts for the greater problem [11]. On the other hand, the contribution of higher energy peaks is important in obtaining an appropriate fit to the experimental glow curve of these specific TLDs. Although some authors [23,24] ignore this glow peak in their analysis, Bos et al. [25] reported that the necessity of including peak 5a (peak 6) in the deconvolution procedures appears important for several TLDs. Kitis and Otto [22] isolated this peak from other neighboring peaks via a specific thermal handling between 140 and 160 °C. They reported very high activation energy ($E > 3$ eV) and frequency factor

Table 1. Calculated activation energies obtained according to GOK and Lambert equations for the sake of comparison.

Material		peak 1			peak 2			peak 3			peak 4			peak 5			peak 6			peak 7			peak 8		
		GOK	Lambert W-function	*Devia.* %	GOK	Lambert W-function	*Devia.* %	GOK	Lambert W-function	*Devia.* %	GOK	Lambert W-function	*Devia.* %	GOK	Lambert W-function	*Devia.* %	GOK	Lambert W-function	*Devia.* %	GOK	Lambert W-function	*Devia* %	GOK	Lambert W-function	*Devia.* %
Lithium fluoride (Li natural) LiF: Mg, Ti	**TLD100**	0.61	0.69	13.80	1.03	1.04	0.48	1.34	1.31	2.50	1.67	1.68	0.11	1.99	1.95	2.17	2.90	2.13	26.55	2.11	2.52	19.62	2.34	2.65	13.27
Lithium fluoride (^{6}Li) LiF: Mg, Ti	**TLD600**	0.60	0.72	20.06	1.18	1.22	2.53	1.35	1.31	3.21	1.70	1.80	5.60	2.23	2.05	7.91	3.20	2.50	21.88	1.90	2.80	47.30			
Lithium fluoride (^{7}Li) LiF: Mg, Ti	**TLD700**	0.60	0.70	16.52	1.18	1.20	1.42	1.45	1.42	2.39	1.65	1.67	1.34	2.26	2.15	4.93	3.10	2.50	19.36	1.80	2.84	57.83			
Aluminum oxide (Al_2O_3)	**TLD500**	0.77	0.80	3.50	1.11	1.23	10.77	1.27	1.28	0.71															
Beryllium oxide (BeO)		0.79	0.79	0.06	1.08	1.11	2.82	1.15	1.14	1.16															

Table 2. Estimated kinetic order parameters, b, and retrapping ratio, R, for all peaks according to GOK and Lambert W-function approximations, respectively.

Material		peak 1		peak 2		peak 3		peak 4		peak 5		peak 6		peak 7		peak 8	
		GOK (b)	Lambert W-function (R)	GOK (b)	Lambert W-function (R)	GOK (b)	Lambert W-function (R)	GOK (b)	Lambert W-function (R)	GOK (b)	Lambert W-function (R)	GOK (b)	Lambert W-function (R)	GOK (b)	Lambert W-function (R)	GOK (b)	Lambert W-function (R)
Lithium fluoride (Li natural) LiF: Mg, Ti	TLD100	1.00	0.04	1.00	0.01	1.13	0.06	1.07	0.12	1.18	0.08	1.00	0.04	1.00	0.01	2.00	0.90
Lithium fluoride (^{6}Li) LiF: Mg, Ti	TLD600	1.00	0.06	1.00	0.01	1.08	0.52	1.26	0.24	1.09	0.06	1.00	0.01	2.00	0.90		
Lithium fluoride (^{7}Li) LiF: Mg, Ti	TLD700	1.00	0.08	1.00	0.01	1.16	0.09	1.19	0.24	1.07	0.06	1.78	0.79	1.92	0.88		
Aluminum oxide (Al_2O_3)	TLD500	1.00	0.08	1.28	0.06	1.00	0.00										
Beryllium oxide (BeO)	5.	1.00	0.01	1.00	0.01	1.00	0.01										

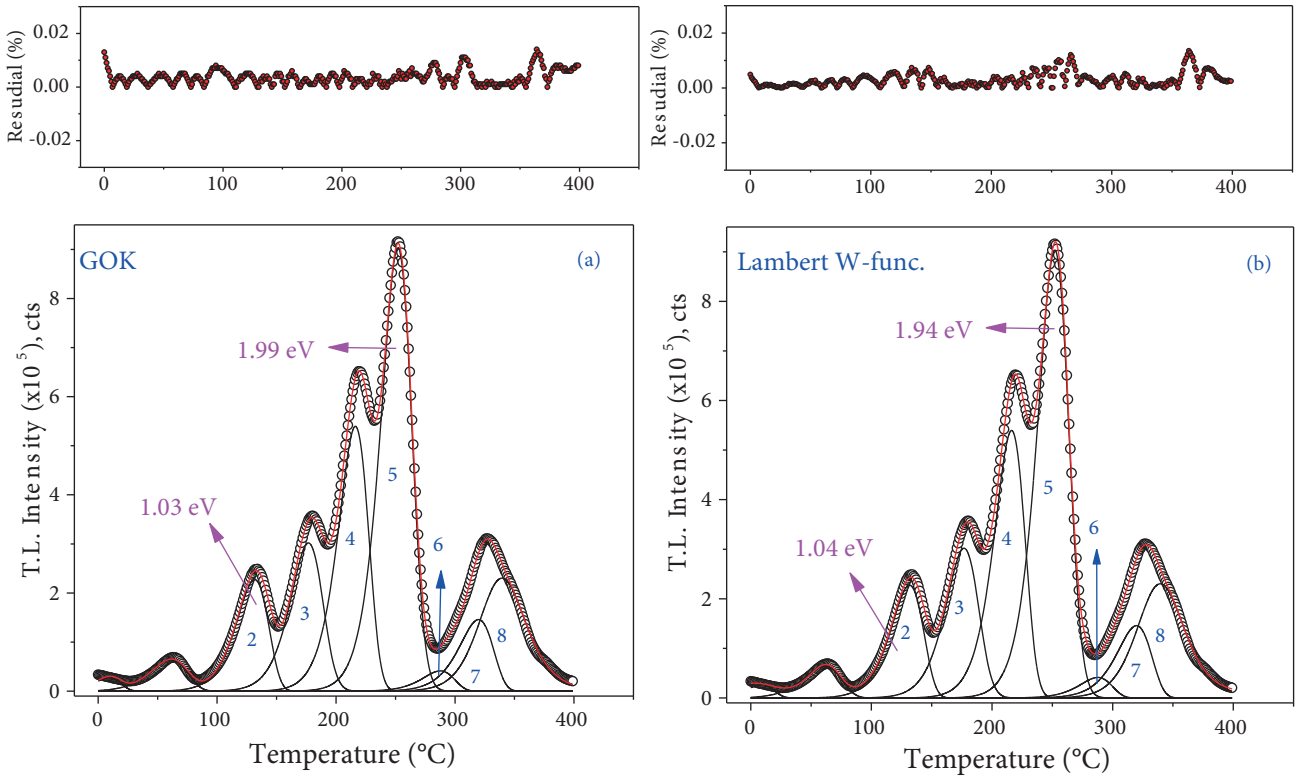

Figure 1. The glow-curve deconvolution analysis of TLD100 dosimeter irradiated by 10 Gy of ^{90}Sr–^{90}Y source. The FOM for the analysis were 1.8% and 1.4% for (a) GOK and (b) Lambert W-function, respectively.

($s > 10^{30}$ s^{-1}) values for this glow peak. However, this high activation energy is clearly affected by the previous annealing temperature.

In general, as expected from Figures 1–3 (at least up to peak 5), the analysis and the kinetic parameter values of the GOK and Lambert W-function are very similar to each other. Still, despite a total number of eight peaks required to fit the glow curve of TLD100, one fewer peak is required in order to fit the TLD600 and TLD700, namely just seven peaks. As for the cases of Al_2O_3:C and BeO, illustrated in Figures 4 and 5, respectively, deconvolution analyses have estimated energies showing consistent values with the related literature findings [26,27].

These materials are abundantly available as chemically inactive and as ceramic materials and are more sensitive than LiF-based dosimeters. In particular, TL peak number 2 is significant for dosimetry fields for both materials. The corresponding calculated energies are 1.11 ± 0.06 eV and 1.23 ± 0.04 eV for Al_2O_3:C and 1.08 ± 0.05 eV and 1.11 ± 0.05 eV for BeO for GOK and Lambert W-function, respectively.

To the best of the author's knowledge, Eq. (4), with a comparison to Eq. (1), is mutually examined for the first time regarding deconvolution analysis of various TL dosimeters in the literature. For each TL peak the R value, being related to the real retrapping ratio, and its counterpart b value in the GOK model are shown in Table 2 for all experimental TL curves.

For LiF-based dosimeters, as energies of Table 1 yield, a good agreement can be observed from the second peak to the fifth peak between the GOK and Lambert approaches. However, for peaks 6–8 differences in activation energy values rise up to 25%, which could be related to increasing retrapping ratios in the

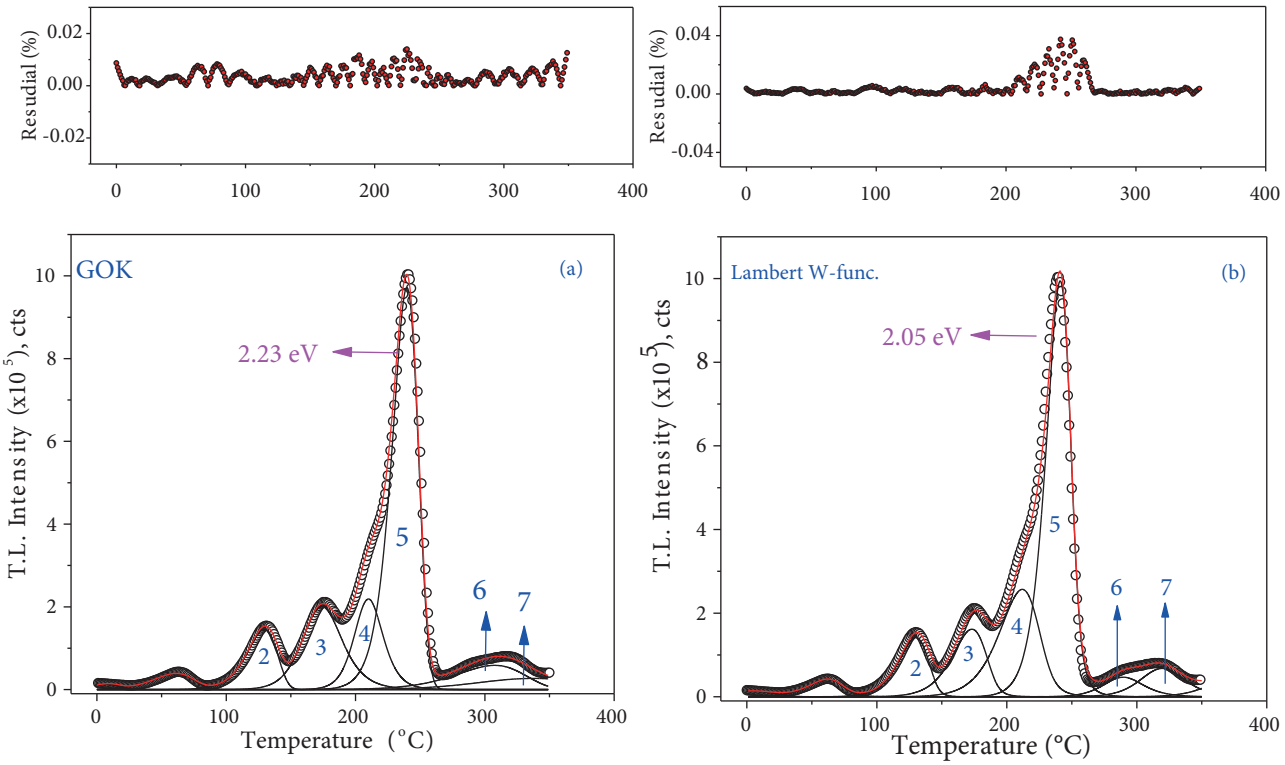

Figure 2. The glow-curve deconvolution analysis of TLD600 dosimeter irradiated by 10 Gy of ^{90}Sr–^{90}Y source. The FOM for the analysis were 1.9% and 1.3% for (a) GOK and (b) Lambert W-function, respectively.

high temperature region. This is a common experimental result when higher (than 1) order of kinetics is yielded. In particular, the GOK model cannot work properly on solids with higher retrapping probability than recombination. Otherwise, the GOK and Lambert W-function approaches have good agreement at 0.06%–10% difference in the case of Al_2O_3:C and BeO crystals.

In respect of retrapping ratio, b and R values can be evaluated and could be considered indicative. The former is related to $b^{b/(b-1)}$ as mentioned in Eq. (1). Furthermore, all model expressions fail when the retrapping probability becomes greater than the recombination probability. The latter is related to the A_n/A_m ratio; the corresponding border conditions were discussed in the paper by Kitis and Vlachos [10].

As presented in Table 2, there is a constrained correlation observed among the retrapping ratios for LiF-based dosimeters; this effect could be attributed to the peak coincidence for both models. However, b and R values are correlated and indicate the first order of kinetics for Al_2O_3:C and BeO dosimeters without overlapped peaks.

In addition to the abovementioned results, although residual signals are more or less the same, some differences were noticed between calculated FOM values. The use of the Lambert W-function results in FOM values with better accuracy in the high temperature area at all peaks. The reason lies in the fact that the exponential integral component of the original TL equation in the case of GOK is calculated numerically. On the other hand, the Lambert approach uses analytical solutions that bring about better fits at the higher temperature part of the peaks as at this part the exponential integral component becomes dominant. A deconvolution example for the BeO crystal is presented in Figures 6a and 6b, which are in logarithmic scale. Although both equations gave good fits with experimental data, they have small differences with FOMs of about

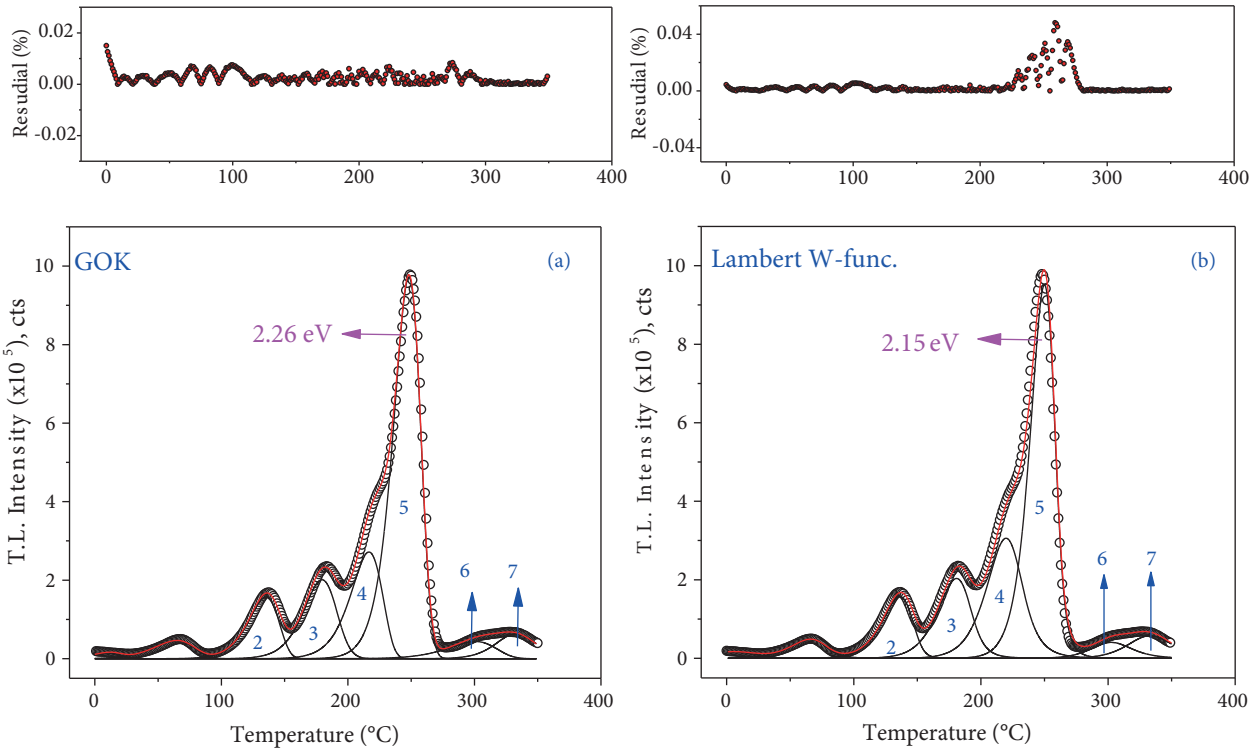

Figure 3. The glow-curve deconvolution analysis of TLD700 dosimeter irradiated by 10 Gy of ^{90}Sr–^{90}Y source. The FOM for the analysis were 2.4% and 1.8% for (a) GOK and (b) Lambert W-function, respectively.

1%–2%. Pointing out similar observations in the paper by Kitis et al. [12], small divergence at the glow peak ending part can clearly be seen because the GOK glow peak appears to decay more quickly to zero related to the numerical solution of the exponential integral (2nd) part of the real TL equation. This situation is also indicated when comparing MOK and GOK by Kitis et al. [28]. Furthermore, model expression fails when the retrapping probability becomes greater than the recombination probability as indicated by Yazıcı [29].

The differences between two expressions are curbed at the higher temperatures end of the TL glow peaks indicated by the arrows on Figures 6a and 6b. The disparity between GOK and Lambert W-function solutions at higher temperature (2nd) parts of TL glow curves can be based on various factors regarding the solid state structure of luminescent materials. One factor might be related to the expression of the signal by means of analytical solution types as mentioned in the manuscript. Although the GOK approach uses the empirical solution, the Lambert W-function uses a totally analytical solution. Another factor could be related to the retrapping ratio while determining the kinetic order of expressions. Furthermore, this difference could happen on account of substantial buildup of free electrons in the conduction band thanks to the relaxation rates (retrapping and recombination) not being able to cope with the excitation rate at high temperatures of glow peaks, depending on concentration and the cross-section values of the input parameters [30]. Besides the aforementioned remarks, the differences in solutions can arise from electron-hole recombination processes through the band structure. Namely, localized and delocalized transitions across the crystals could affect limits of expressions in various parts of heating points, which has been thoroughly discussed for numerous thermal and optical stimulation types in recent years within the luminescence community.

Compared to the experimental results of various natural and artificial luminescence emitting materials,

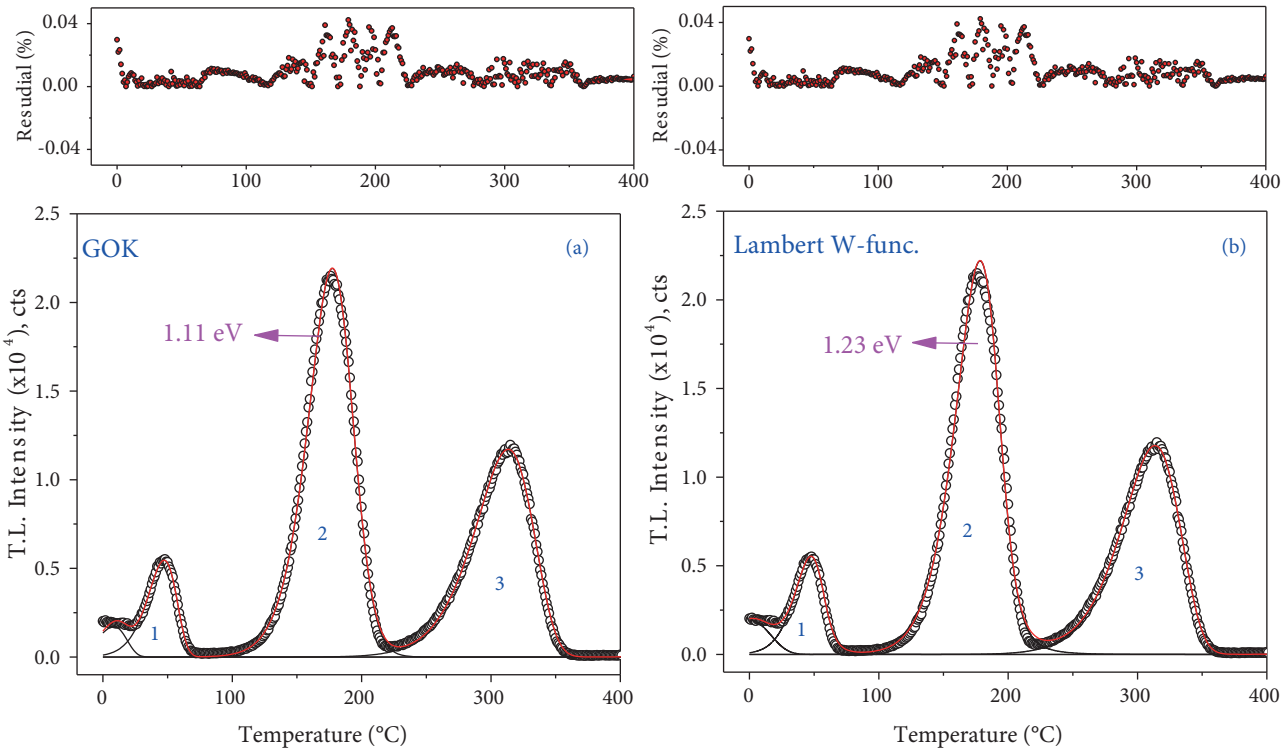

Figure 4. The glow-curve deconvolution analysis of TLD500 dosimeter irradiated by 3 Gy of ^{90}Sr–^{90}Y source. The FOM for the analysis were 2.2% and 1.6% for (a) GOK and (b) Lambert W-function, respectively.

further simulation applications dealing with trap-charge mechanism could be significant to understand the physics-based details of the Lambert W-function solution on the luminescence emissions of solids.

Moreover, thermal quenching, which is linked to the competition between nonradiative and radiative transitions into the ground state of the recombination center resulting in the loss of luminescence efficiency with the augmentation of temperature [31], might affect the intensity of the TL signal. In particular, for Al_2O_3:C and BeO, thermal quenching can play an important role in the kinetic parameters. The retrapping parameters (b or R) and the determined energy values are yielded smaller than their real values; similar results were previously presented by Dallas et al. [32].

Regarding the main dosimetric peak of BeO (2nd peak of Figures 6a and 6b) the kinetic parameters derived from CGCD are: (a) GOK method: $T_m = 191 \pm 0.5$ °C, E = 1.08 eV, and b = 1.001; (b) Lambert method: $T_m = 190 \pm 0.5$ °C, E = 1.11 eV, and R = 0.0131. In conclusion, that good agreement between the regular equation count on GOK and the TL peak expressions depended on the Lambert (OTOR) solution.

The frequency factor (s) stands as a parameter that is associated with the frequency of the atomic vibrations in the lattice. According to the deconvolution results, which are presented in tabulated form in Table 3, frequency factors of the main dosimetric peaks of dosimeters exploit the compatibility of the two mathematical approaches that were applied. Frequency factors estimated from the Lambert approach show higher results than those calculated according to the GOK approach. This disparity could be related to the mathematical assumptions of both models.

The calculated frequency factor values (in the range of $\sim 10^{18}$ to $\sim 10^{23}$ s^{-1}) for the mean dosimetric peak of LiF-based dosimeters, peak 5, are in good agreement with both Kitis et al. [33], who determined them

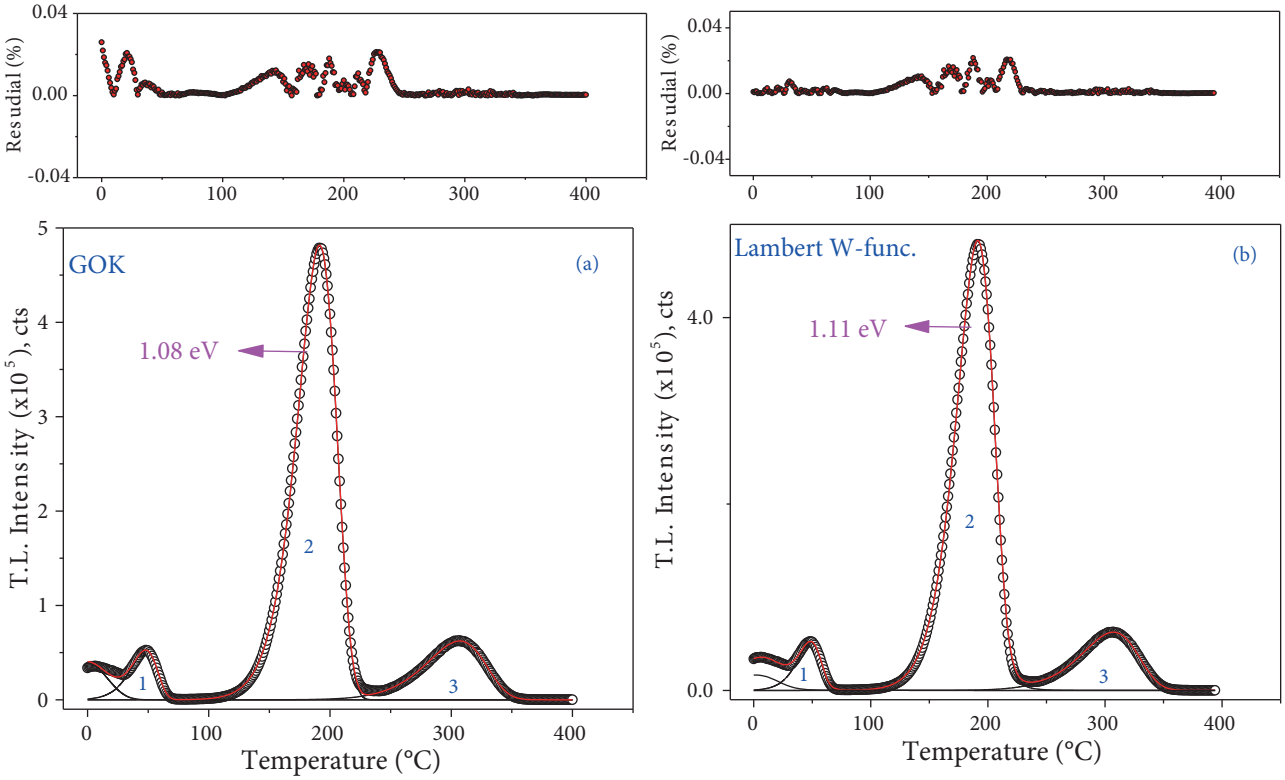

Figure 5. The glow-curve deconvolution analysis of BeO dosimeter irradiated by 5 Gy of ^{90}Sr–^{90}Y source. The FOM for the analysis were 2.1% and 1.3% for (a) GOK and (b) Lambert W-function, respectively.

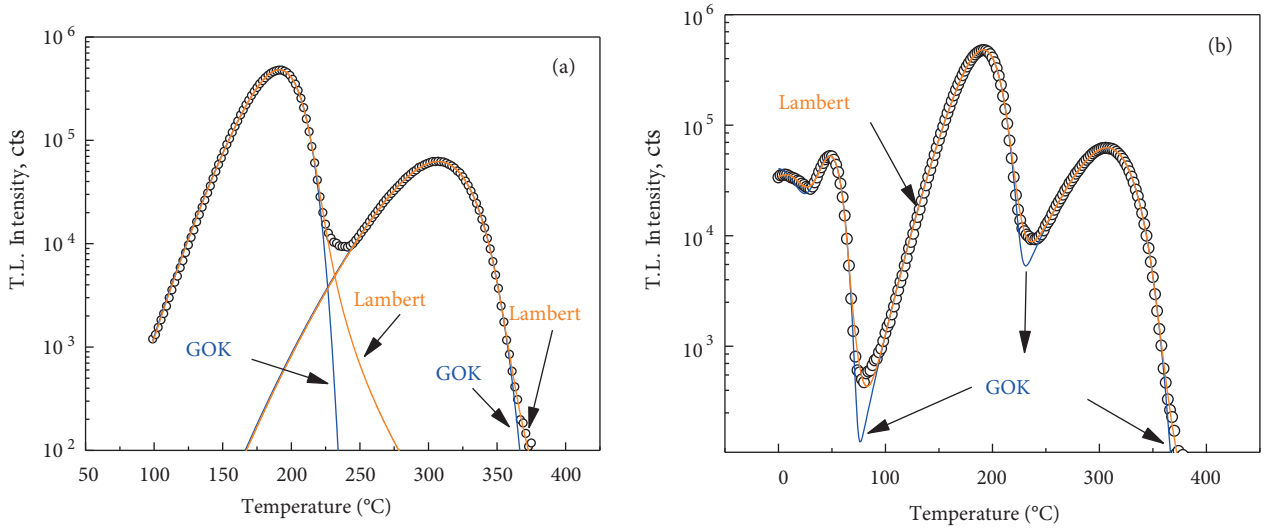

Figure 6. TL glow-curve deconvolution of BeO using Eq. (1) and Eq. (3); both approaches gave appropriate fit. The figure includes the dosimetric main TL peaks leading to both equations. The differences between the two equations are indicated by the corresponding arrows. In the figures, straight line represents general order kinetics and the Lambert (OTOR) whereas open circles indicate experimental. (a) individual deconvolved peaks, (b) sum of the peaks according to both expressions.

Table 3. Estimated frequency factors of main dosimetric peaks using both GOK and Lambert W-function approximations.

Material		Frequency factors of main dosimetric peaks, s (s^{-1})	
		GOK approach	Lambert W-function approach
Lithium fluoride (Li natural) LiF: Mg, Ti	TLD100	1.09×10^{18}	1.65×10^{22}
Lithium fluoride (^{6}Li) LiF: Mg, Ti	TLD600	1.79×10^{22}	1.12×10^{23}
Lithium fluoride (^{7}Li) LiF: Mg, Ti	TLD700	7.40×10^{20}	2.20×10^{22}
Aluminum oxide (Al_2O_3)	TLD500	1.77×10^{11}	4.44×10^{13}
Beryllium oxide (BeO)		3.09×10^{11}	1.23×10^{14}

as $\sim 10^{20}$ s^{-1}, and Sadek et al. [34], who reported values in the range of 10^{19}–10^{21} s^{-1}. Furthermore, calculated frequency factors of BeO, which are $\sim 10^{11}$ s^{-1} and $\sim 10^{14}$ s^{-1}, are also acceptably compatible with average values reported by Bacci et al. [26]. As for TLD500 results, $\sim 10^{11}$ and $\sim 10^{13}$ s^{-1}, different results have been reported in the literature ranging from $\sim 10^{11}$ to $\sim 10^{16}$ s^{-1} depending on the calculation method [35].

It has been mentioned that both the GOK equation of Eq. (1) and the Lambert equation of Eq. (4) are based on the OTOR model, where the order of kinetic is associated only with the ratio of the retrapping and recombination probabilities R. Thus, the generated Lambert equation could be a promising alternative method for determining activation energies and characterizing the solids with TL.

4. Conclusions

Deconvolution analysis of glow curves corresponding to various established dosimetric materials was carried out using the GOK and recently developed Lambert W-function approaches. The comparison of energies was displayed in terms of both approximations as well as retrapping ratios. The energy values of the main dosimetric peaks were calculated as 1.94 ± 0.06, 2.05 ± 0.05, 2.15 ± 0.06, 1.23 ± 0.06, and 1.11 ± 0.05 eV for TLD100, TLD600, TLD700, TLD500, and BeO materials, respectively. Moreover, frequency factors of the Lambert approach were found to be higher than those of the GOK approach. Finally, the Lambert solution is superior to the GOK method, tending much faster to zero, considering the second part of the TL peaks.

In conclusion, the Lambert W-function, which is the core of the OTOR model, is a useful approach for decomposing overlapped glow peaks in material characterization. In addition, it is a promising method to unearth the obscurity of the trap-charge mechanism of solids using physical meaningfulness of $R = A_n/A_m$ (retrapping ratio) replacing the kinetic order b parameter in the GOK model.

Nomenclature

E trap depth or activation energy (eV)
R retrapping ratio (A_n/A_m) (only for W)
A_n probability of retrapping (cm^{-3} s^{-1})
A_m recombination probability (cm^{-3} s^{-1})
S frequency factor (s^{-1})
B kinetic order (only for GOK)
N concentrations of electrons (cm^{-3})
N electron trap concentration (cm^{-3})
β heating rate (°C/s)
I intensity
I_m maximum peak intensity

k Boltzmann constant
T absolute temperature (K)
T_m maximum peak temperature
n_0 concentrations of free electrons (cm^{-3})
W Lambert W-function

References

[1] McKeever, S. W. S. *Thermoluminescence of Solids*; Cambridge University Press: Cambridge, UK, 1985.

[2] Bos, A. J. J. *Radiat. Meas.* **2006**, *41*, 45-56.

[3] Randall, J. T.; Wilkins, M. H. F. *Proc. R. Soc. London.* **1945**, *184*, 366-389.

[4] Randall, J.T.; Wilkins, M. H. F. *Proc. R. Soc. London.* **1945,** *184*, 390-407.

[5] Garlick, G. F. J.; Gibson, A. F. *Proc. Phys. Soc.* **1948**, *60*, 574-589.

[6] May, C. E.; Partridge, J. A. *J. Chem. Phys.* **1964**, *40*, 1401-1415.

[7] Kitis, G.; Gomez-Ros, J. M.; Tuyn, J. W. N. *J. Phys. D.* **1998**, *31*, 2636-2641.

[8] Pagonis, V.; Furetta, C.; Kitis, G. *Numerical and Practical Exercises in Thermoluminescence*; Springer: Berlin, Germany, 2006.

[9] Chen, R.; McKeever, S. W. S. *Theory of Thermoluminescence and Related Phenomena*; World Scientific: Singapore, 1997.

[10] Kitis, G.; Vlachos. N. D. *Radiat. Meas.* **2013**, *48*, 47-54.

[11] Sadek, A. M.; Khamis, F.; Polymeris, G. S.; Carinou, E.; Kitis, G. *Phys. Status Solidi C* **2017**, *14*, 1-10.

[12] Kitis, G.; Polymeris, G. S.; Sfampa, I. K.; Prokic, M.; Meriç, N.; Pagonis, V. *Radiat. Meas.* **2016**, *84*, 15-25.

[13] Furetta, C.; Kitis, G.; Kuo, C. H. *Nucl. Instr. Meth. Phys. Res. B* **2000**, *160*, 65-72.

[14] Pagonis, V.; Kitis, G. *Radiat. Prot. Dosim.* **2001**, *95*, 225-229.

[15] Pagonis, V.; Mian, S.; Kitis, G. *Radiat. Prot. Dosim.* **2001**, *93*, 11-17.

[16] Lucas, A. C. In: *Applied Thermoluminescence Dosimetry*; Oberhofer, M., Scharmann, A., Eds. Pergamon Press, Oxford, UK, 1981.

[17] Sadek, A. M. *Nucl. Instrum. Methods Phys. Res. A* **2013**, *712*, 56-61.

[18] Sadek, A. M.; Eissa, H. M.; Basha, A. M.; Carinou E.; Askounis P.; Kitis G. *Radiat. Isot.* **2015**, *95*, 214-221.

[19] Sadek, A. M.; Eissa, H. M.; Basha, A. M.; Kitis, G. *Phys. Status Solidi B* **2014**, *252*, 721-729.

[20] Sadek, A. M.; Eissa, H. M.; Basha, A. M.; Kitis, G. *J. Lumin.* **2014**, *146*, 418-423.

[21] Balian, H. G.; Eddy, N. W. *Nucl. Instr. Meth.* **1977**, *145*, 389-395.

[22] Kitis, G.; Otto, T. *Nucl. Instrum. Methods Phys. Res B* **2000**, *160*, 262-273.

[23] Gartia, R. K.; Dorendrajit Singh S. *Phys. Status Solidi A* **1993**, *135*, 83-86.

[24] Abd El-Hafez, A. I.; Yasin, M. N.; Sadek, A. M. *Nucl. Instrum. Methods A* **2011**, *637*, 158-163.

[25] Bos, A. J. J.; Piters, T. M.; De Varies, W.; Hoogenboom J. E. *Radiat. Prot. Dosim.* **1990**, *33*, 7-10.

[26] Bacci, C.; Bernardini, P.; Damilano, A.; Furetta, C.; Rispoli, B. *J. Phys. D: Appl. Phys.* **1989**, *22*, 1751-1757.

[27] Nieto, J. A.; Vega, C. A.; Montalvo, T. R.; Cabrera, E. T. *Appl. Radiat. Isot.* **2016**, *108*, 8-11.

[28] Kitis, G.; Furetta, C.; Prokic, M.; Prokic, V. *J. Phys. D Appl. Phys.* **2000**, *33*, 1252-1262.

[29] Yazıcı, A. N. *8th International Conference on Luminescence and ESR Dosimetry (LumiDoz8),* Book of Abstracts, 27–29 August 2014, p. vi.

[30] Sunta, C. M. *Unraveling Thermoluminescence*; Springer: Berlin, Germany, 2014.

[31] Curie D. *Luminescence in Crystals*; Methuen: London, UK, 1963.

[32] Dallas, G. I.; Afouxenidis, D.; Stefanaki, E. C.; Tsagas, N. F.; Polymeris, G. S.; Tsirliganis, N. C.; Kitis, G. *Phys. Status Solidi A* **2008**, *205*, 1672-1679.

[33] Kitis, G.; Kiyak, N. G.; Polymeris, G. S. *Nucl. Instrum. Methods Phys. Res B* **2015**, *359*, 60-63.

[34] Sadek, A. M.; Eissa, H. M.; Basha, A. M.; Carinou, E.; Askounis, P.; Kitis, G. *Appl. Radiat. Isot.* **2015**, *95*, 214-221.

[35] Yüksel, M.; Portakal, Z. G.; Dogan, T.; Topaksu, M.; Unsal, E. *RAD 2015 Conference Proceedings: 3rd Conference on Radiation and Applications in Various Fields of Research*, Budva, Montenegro 8–12 June 2015; RAD Association; Budva, 2015, *3, 1*, p. 387-392.